

Periodic Research

Investigations of Synthetic $Zn_{1-x}Cd_xO$ Nanocrystals for Photocatalytic Applications

Abstract

Metal oxide semiconductor nanostructures have attracted great interest due to size tunable photo-physical and photo-chemical characteristics. The doping of transition elements in the metal oxides can affect the photocatalytic activity to large extent by altering excited charge carrier dynamics. In the present paper, $Zn_{1-x}Cd_xO$ ($0 \leq x \leq 0.1$) nanostructures have been synthesized by using a facile co-precipitation method. Crystallographic and morphological characterizations of synthesized nanomaterials have been reported by powder X-ray diffractometer and transmission electron microscope, respectively. Recorded diffractograms reveal the successful substitution of Cd^{2+} in the ZnO at the lattice positions and the average particle size calculated has been ~25 nm from electron micrographs. The XRD patterns reveal the formation of a wurtzite (hexagonal) crystal structure with crystallite size in the range of 16.53–20.12 nm. Energy dispersive spectroscopic analyses confirm the presence of cadmium in Cd-doped ZnO nanostructures. The UV–Visible absorption spectra showed a shift in absorption edge with an increase in Cd dopant concentration in ZnO. The PL spectra show near band edge emission and defect-related visible emission band. Photocatalytic activity of the synthesized nanomaterials has been tested using methylene blue (MB) dye as a test contaminant in aqueous media under UV light irradiation. Photo-catalytic activity dependence on zinc and cadmium concentration in II–VI ceramic semiconductor nanostructures has been studied in detail. These nanomaterials seem to be good candidates for opto-electronic industrial applications as well as efficient nano-photocatalysts.

Keywords: Nanocrystals, Crystallography, Morphology, Photoluminescence; Photo-Catalytic Activity, Pollution Control.

Introduction

Environmental pollution and energy crisis are two serious threats in our society. Therefore numerous scientists are focused on to explore possible solutions and seeking energy from different sources. Semiconductor photocatalysts are promising tools for harvesting solar energy and solve the global problem of the energy crisis and environmental pollution. Photocatalytic activity is a very active field of pollution control. In particular, dye degradation of water pollutants is essential for wastewater treatment due to its low cost, high efficiency and production of no other secondary pollutants [1]. Semiconductor photocatalyst attracted more attention in the field of photocatalysis due to their excellent degradation efficiency for various pollutants. Over the past decades, zinc oxide (ZnO) is the most studied and efficient material for photocatalytic applications because of their high stability and a low risk to the environment [2–5]. The hexagonal wurtzite ZnO is a n-type II–VI semiconductor compound characterized by the wide direct band gap of 3.37 eV with large exciton binding energy of 60 meV at room temperature [2]. Due to such interesting properties, ZnO can be used in pigments, gas sensors, optical devices, solar cells, and photocatalysis [6–10]. As ZnO is a wide band semiconductor, it absorbs only in ultraviolet region of the solar spectrum. To increase its utility in the visible region of the solar spectrum and enhance the photocatalytic activity, ZnO can be modified by doping with metal ions [11]. In the case of Cd-doped ZnO nanostructures, Cd^{2+} ion capture photogenerated electrons and restrain recombination of electron and hole, therefore the photocatalytic activity of ZnO material is enhanced [12–14]. The main aim of this research work is to synthesize Cd doped ZnO nanostructures via co-precipitation method. Effect of different concentrations of Cd dopant on the structural, optical, morphological and

Ram Pal

Research scholar,
Dept of Physics,
Punjabi University, Patiala,
Punjab, India

Karamjit Singh

Assistant Professor,
Dept of Physics,
Punjabi University, Patiala,
Punjab, India

H. S. Bhatti

Ex. Dean Physical Sciences &
Head,
Dept of Physics,
Punjabi University, Patiala,
Punjab, India

E: ISSN No. 2349-9435

photocatalytic activity of ZnO nanostructures have been systematically studied.

Experimental Section

Materials

Zinc acetate dihydrate $[\text{Zn}(\text{CH}_3\text{COO})_2 \cdot 2\text{H}_2\text{O}]$, cadmium acetate dehydrate $[\text{Cd}(\text{CH}_3\text{COO})_2 \cdot 2\text{H}_2\text{O}]$ and sodium hydroxide (NaOH) were used without further purification.

Sample Preparation

In a typical synthesis, 0.5 M of $\text{Zn}(\text{CH}_3\text{COO})_2 \cdot 2\text{H}_2\text{O}$ and different weight percentage (0.005, 0.05 and 0.1%) of $\text{Cd}(\text{CH}_3\text{COO})_2 \cdot 2\text{H}_2\text{O}$ was dissolved in 50 ml of distilled water. A simultaneously appropriate amount of aqueous solution of NaOH was added gradually in the main mixture to maintain the pH of resultant solution at 12. Solutions of 0.5 M zinc acetate, 0.5 M sodium hydroxide, and 1 M cadmium acetate were prepared in separate beakers. Then zinc and cadmium precursor solutions were mixed in the stoichiometric proportion under vigorous stirring, before drop wise addition of oxide precursor. The

Results and Discussion

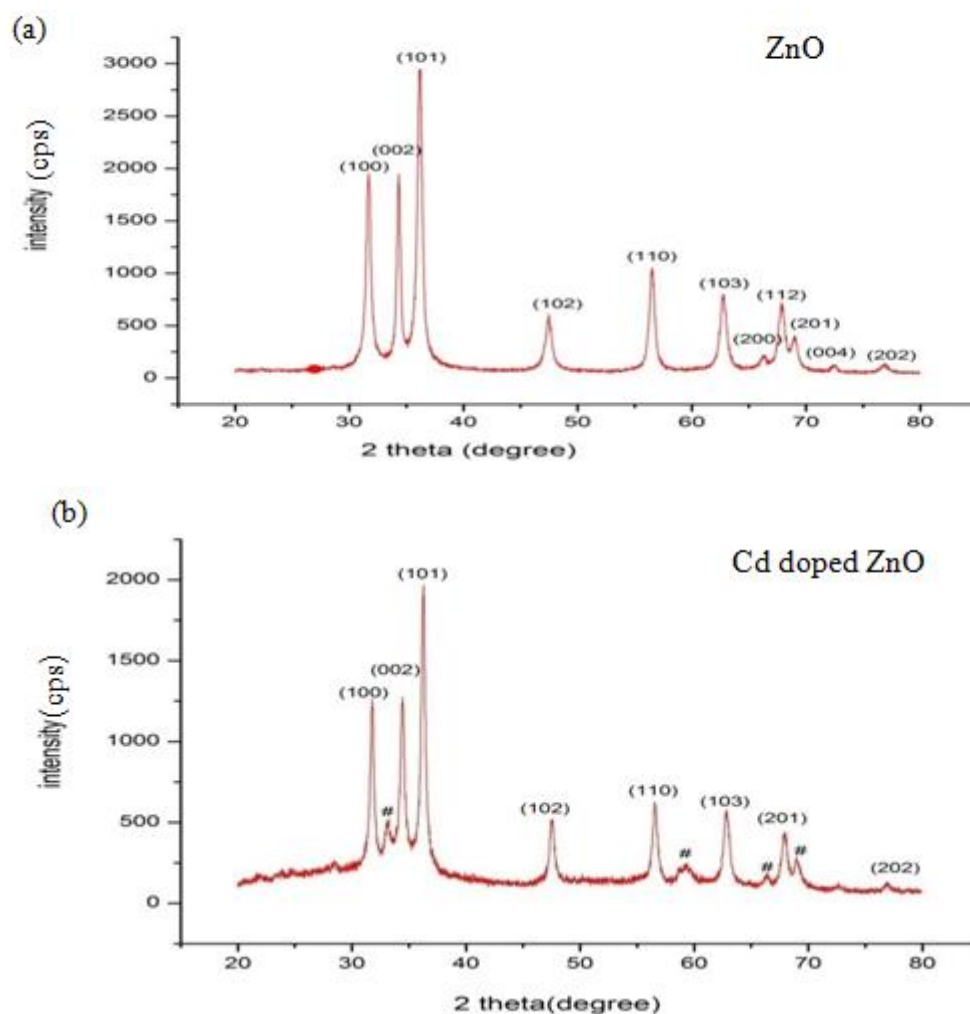
Crystallographic Studies

resulting precipitates were centrifuged and dried in vacuum oven for 10 to 12 h continuously.

Characterizations

Intrinsic and extrinsic ZnO samples were studied for crystallographic analysis using X-Ray Diffractometer (XRD) Rigaku Miniflex model using $\text{Cu K}\alpha_1$ radiation with $\lambda = 1.5418\text{\AA}$. The optical properties were conducted using UV Vis. absorption spectrophotometer. The morphological studies of synthesized pure and doped ZnO nanostructures were performed by transmission electron microscope [Hitachi (H-7500) TEM]. The elemental compositions of the synthesized ZnO samples was examined by using energy dispersive spectroscopy (EDS). The room-temperature photoluminescence spectra were recorded on a fluorescence spectrophotometer. Photocatalytic activity of these nanocrystalline materials was tested using an indigenous UV/visible light reactor specially designed for these studies in our research laboratory.

Figure 1 XRD pattern $\text{Zn}_{1-x}\text{Cd}_x\text{O}$ ($0 \leq x \leq 0.1$) nanocrystals



(a) ZnO (b) $\text{Zn}_{0.90}\text{Cd}_{0.10}\text{O}$

Periodic Research

Broad XRD patterns have been recorded for all the synthesized Zn_{1-x}Cd_xO samples, average crystallite size *D* was calculated using the Debye–Scherer equation:

$$D = 0.9\lambda / \beta \cos\theta$$

Where λ is the wavelength of X-ray used, β is the full width at half maximum (FWHM) of diffraction peak, and θ is the Bragg angle [15]. The X-Ray Diffraction (XRD) measurements were carried out using Cu K α 1 radiation ($\lambda = 1.5418 \text{ \AA}$), Figure 1(a) shows one such X-ray diffractogram recorded for ZnO. The XRD patterns of all pure and doped ZnO samples exhibited a typical wurtzite (hexagonal) crystal structure (JCPDS card no. 36-1451). All samples show diffraction peaks at 31.96°, 34.54°, 36.39°, 47.75°, 56.69°, 62.99°, 66.54°, 68.16°, 69.33°, 72.71° and 77.06° corresponding to (100), (002), (101), (102), (110), (103), (200), (112), (201), (004), and (202) planes. Recorded diffraction peaks are broadened due to the nanocrystalline nature of particles. Average

Morphological Analyses

crystallite size calculated from the recorded XRD patterns is approx. 16.53 nm. The recorded XRD patterns of synthesized ZnO nanoparticles are in good agreement with the diffractograms reported in literature [16]. Figure 1(b) shows one such X-ray diffractogram recorded for Zn_{0.90}Cd_{0.10}O. It is clear from the diffractogram that synthesized Zn_{0.90}Cd_{0.10}O samples show a slight shifting of the centre of diffraction peaks toward higher angle compared to pure ZnO. The shifts of the peak indicate a compaction of the unit cell, possibly, because the Cd ions prefer to occupy the interstitial sites. Such a change is expected, because the Cd ion has greater ionic radius compared to Zn ion. The pure phase of the XRD and the slight shift of the peak position imply that the Cd atoms effectively occupy sites in the ZnO lattices. Average crystallite size of synthesized Zn_{0.90}Cd_{0.10}O samples calculated from the recorded XRD patterns is approx. 20.4nm.

Figure 2 TEM image of Zn_{1-x}Cd_xO (0 ≤ x ≤ 1) Nanocrystals

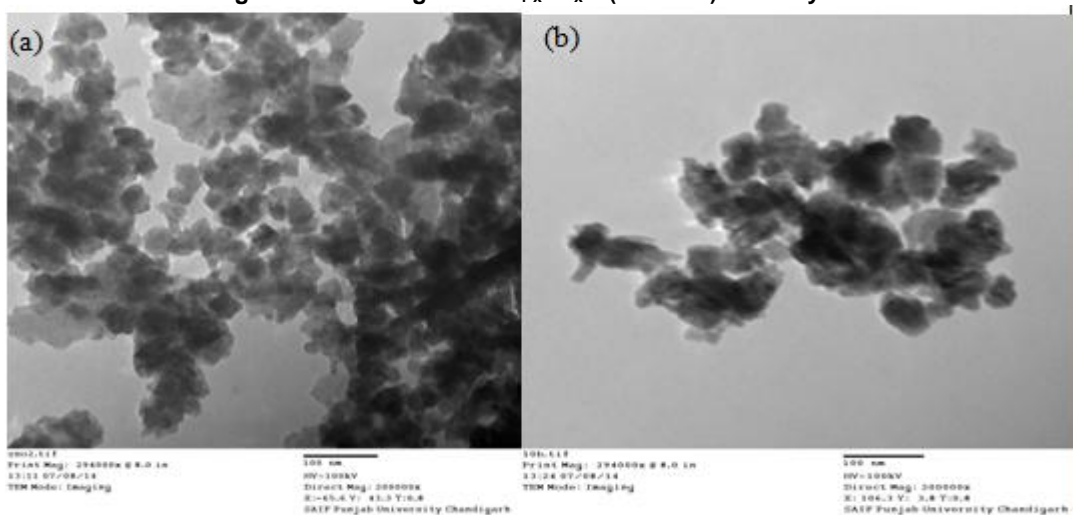
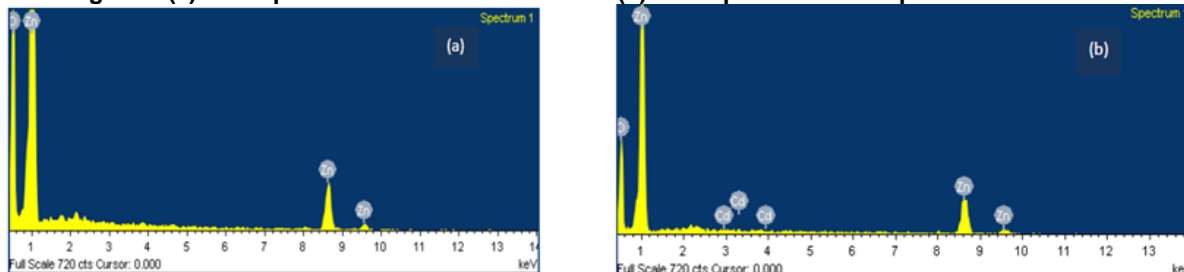


Figure 2 (a&b) shows the TEM micrographs recorded for Zn_{1-x}Cd_xO nanocrystals. Average particle size calculated from electron micrograph is ranging

approximately between 22-25 nm, which is different to the average crystallite size determined by XRD. So, all the synthesized particles are poly nanocrystals.

Elemental Analysis

Figure 3 (a) EDX spectra of ZnO nanostructures (b) EDX spectra of Cd doped ZnO nanostructures



Element	Weight%	Atomic%
O K	26.57	59.65
Zn L	73.43	40.35
Totals	100.00	

Element	Weight%	Atomic%
O K	25.08	57.84
Zn L	74.44	42.00
Cd L	0.48	0.16
Totals	100.00	

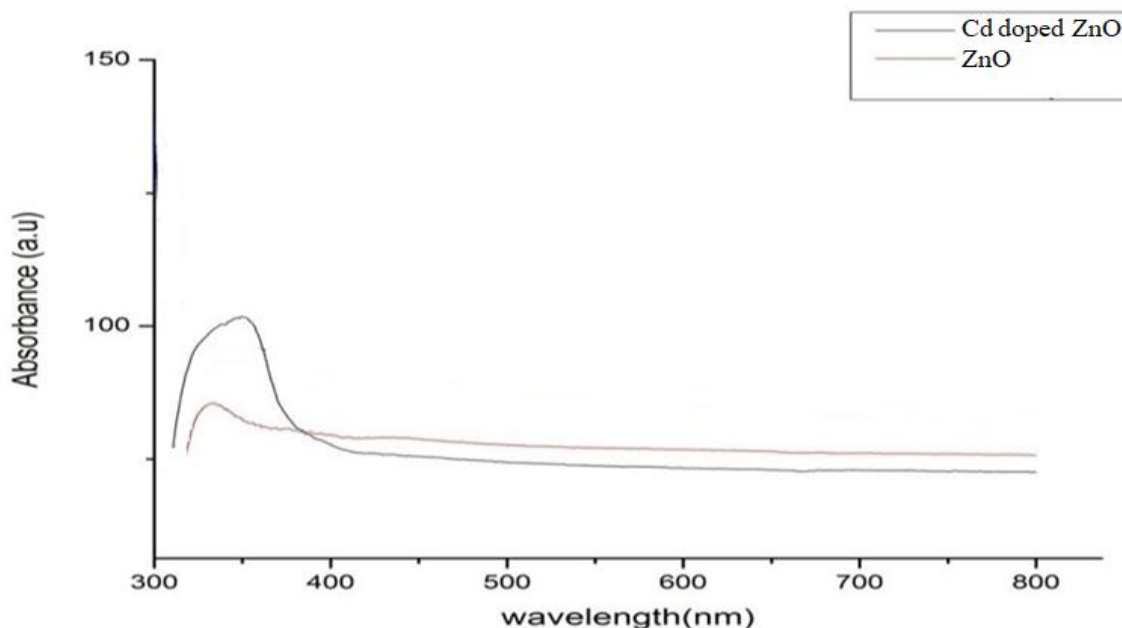
Periodic Research

The elemental composition was determined by energy dispersive spectroscopy (EDS) techniques and color mapping analysis. Peaks confirmed the presence of the elements Zn & O for ZnO, no extra peak was observed, which indicates that the synthesized ZnO nanostructures are highly pure. EDS spectra [Fig. 3 (a)] recorded for pure ZnO

nanostructures show 26.57 wt % (59.65 at %) and 73.43 wt % (40.35 at %) of zinc and oxygen, respectively. Fig. 3(b) reveal the formation of Cd doped ZnO, 74.44 wt % (42.01 at %), 25.08 wt % (57.84 at %) and 0.48 wt % (0.16 at %) are the observed concentration values for zinc, oxygen and cadmium, respectively.

Optical Properties

Figure 4 Absorption spectra of Zn_{1-x}Cd_xO nanocrystals

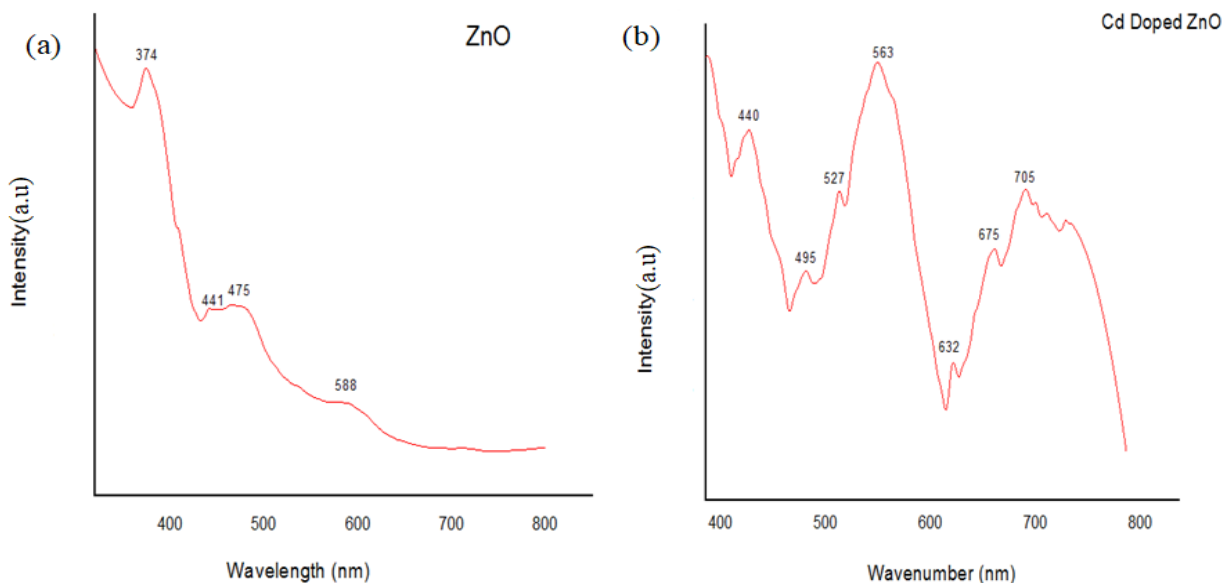


The UV-visible spectroscopy provides the estimation of band gap energy for synthesized nanoparticles. The absorbance spectra of these nanoparticles have been recorded in the range of 300-800 nm. It clearly shows that as augmented the content of "Cd" doping in host lattice, band gap shifts towards higher wavelength. Moreover, sharp, narrow

peak is observed in comparison to broad peak obtained in case of maximum content of Cd substituted in ZnO nanocrystals, which is related with ZnO and a characteristic peak for wide-band gap ZnO[19-21]. The change in the value of E_g depends on various factors such as lattice strain, grain size, carrier concentration, etc.

Photoluminescence Study

Figure 5 (a-b) Photoluminescence spectra of Zn_{1-x}Cd_xO nanocrystals



Energy resolved luminescence spectra shown in Figure 5 have been recorded at room temperature using 344nm and 326 nm excitation. The most probable effect observed to be oxygen vacancy, zinc vacancy, oxygen interstitials and zinc interstitials [2,17, 18]. Figure 5 (a-b) represents the PL spectra of pure ZnO and 10% Cd doped ZnO. The UV emission corresponding to the near-band-edge emission of ZnO originates from excitonic recombination [22, 23]. In case of pure ZnO the first peak observed at 374 nm was a near band edge (NBE) emission and attributed to recombination of photogenerated free electron and hole pair [2]. The weak NBE emission indicates that dominated defect-related emission. The Cd^{2+} dopant may act as an electron acceptor for ZnO and prohibited recombination of photoexcited electron and hole pair. The reduction in electron/ hole recombination rate indicates the decrease in NBE emission of Cd doped ZnO. The emission peak centered at 440 nm (violet) assigned to transition from zinc interstitials to the valence band. In case of violet

Photocatalytic Activity

emission, when electrons were excited up to a sub-band of the conduction band, they can first relax to the $\text{Zn}_{\text{interstitial}}$ state through non-radiative transition and transmit to the valence band. The second peak of pure ZnO lies at 475 nm and in Cd doped ZnO at 495 nm (blue region) attributed to the presence of intrinsic defects in ZnO including O vacancies and Zn interstitials. Shoulder peak lies only in case of pure ZnO at 588 nm (yellow range) whereas in Cd doped ZnO samples emission from the deep defect states is observed in the red region. The different sublevels were generated below the conduction band due to oxygen vacancies. These states act as a recombination center for the electron hole pair that can be ascribed to the transition from extended zinc interstitials state to the valence band. The radiative recombination probability strongly effect the photocatalytic activity potential of the nanocrystals, more are chances of radiative relaxation of excited charge carriers lesser will be the chances of surface charge transfer and hence the photocatalytic activity.

Figure 6 Photodegradation of MB Dye with Different Concentrations of Cd in ZnO Nanocrystals

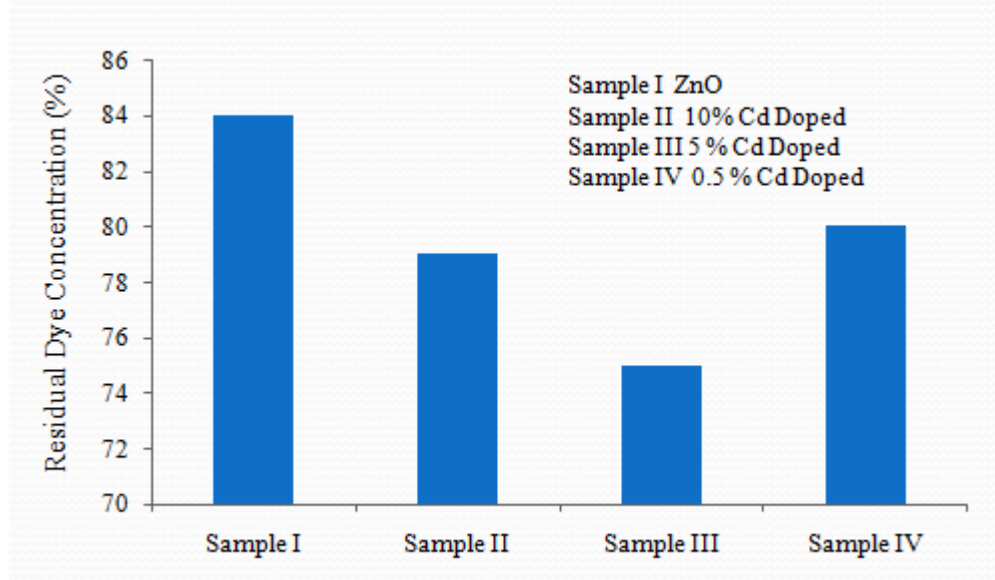


Figure 6 shows photo-degradation of MB dye under UV-radiation exposure of $\text{Zn}_{1-x}\text{Cd}_x\text{O}$ nanocrystals of different size after 90 mins. It can be clearly seen that MB dye is degraded to maximum extent in case of $\text{Zn}_{0.95}\text{Cd}_{0.01}\text{O}$ nanocrystals (as shown in Fig. 6), whereas it is degraded to minimum extent by pure ZnO nanophoto-catalyst. Photoredox chemistry occurring at nanocrystal surface emanates from trapped charge carriers. Incorporation of Cd^{2+} in ZnO nanocrystal lattice significantly influences the photo-catalytic activity. Addition of Cd^{2+} ions lengthens the lifetime of excited charge carriers, which results the enhanced photocatalytic activity. Doping of Cd^{2+} up to optimal concentration increases the interfacial charge transfer probability, due to which photo-catalytic activity of ZnO nanocrystals is enhanced. Moreover, increasing concentration of Cd^{2+} ions beyond optimum value may cause the increased interaction between neighboring Cd^{2+} ions and the

Zn^{2+} luminescence centre that enhances the spin-orbit coupling.

Acknowledgement

The work was technical supported by Sophisticated Instruments Centre (SIC) by Punjabi University, The administration of Physics Department, Faculty of Science, Punjabi University Patiala.

Conclusion

Chemical co-precipitation method is a facile, ecofriendly synthesis technique, which gives good yield of highly pure $\text{Zn}_{1-x}\text{Cd}_x\text{O}$ ($0 \leq x \leq 0.1$) nanocrystals. Crystallographic and morphological studies reveal the wurtzite hexagonal crystal structure with crystallite size in the range of 16.53–20.12 nm. Energy dispersive spectroscopy analysis confirms the presence of cadmium in Cd-doped ZnO samples. Photoluminescence is strongly altered by the addition of dopant ions in the visible region of electromagnetic spectrum. The photocatalytic studies suggest that the

E: ISSN No. 2349-9435

Periodic Research

incorporation of Cd into ZnO significantly enhanced the degradation efficiency of MB dye under UV irradiation. Photocatalytic activity enhances with the addition of Cd²⁺ ions in ZnO nanocrystals upto to optimal concentration. This mechanistic information of photo-catalytic activity dependence on dopant concentration and luminescence quantum yield will significantly contribute to enhance the understanding of photoinitiated processes in semiconductor nanocrystals.

Endnotes

1. R. Dhabbe, A. Kadam, P. Kokare, M. Kokate, P. Waghmare, K. Garadkar, J. Mater. Sci.: Mater. Electron. 26, 554 (2014)
2. K. Ghoderao, S. Jamble, R. Kale, Mater. Res. Exp. 4, 105009(2017)
3. Y. Su, J. Li, Z. Luo, B. Lu, P. Li, RSC Adv. 6, 7403 (2016)
4. P. Korake, R. Dhabbe, A. Kadam, Y. Gaikwad, K. Garadkar, J. Photochem. Photobiol., B 130, 11 (2014)
5. A. Kadam, R. Dhabbe, A. Gophane, T. Sathe, K. Garadkar, J. Photochem. Photobiol., B 154, 24 (2016)
6. A. Ibrahim, R. Kumar, A. Umar, S. Kim, A. Bumajdad, Z. Ansarif, S. Baskoutas, Electrochim. Acta 222, 463 (2016)
7. A. Djuricic, X. Chen, Y. Leung, A. Ng, J. Mater. Chem. 22, 6526 (2012)
8. Z. Zang, A. Nakamura, J. Temmyo, Opt. Express 21, 11448 (2012)
9. Y. Wu, J. Yun, L. Wang, X. Yan, Cryst. Res. Technol. 48, 145(2013)
10. X. Yu, F. Dong, B. Dong, L. Liu, Y. Wu, Adv. Mater. Lett. 8, 393 (2017)
11. Y. Zhai, J. Li, X. Fang, X. Chen, F. Fang, X. Chu, Z. Wei, X. Wang, Mater. Sci. Semicond. Process. 26, 225 (2014)
12. Y. Wang, P. Thomas, P. Brien, J. Phys. Chem. B 110, 21412 (2006)
13. S. Zhou, X. Meng, X. Zhang, X. Fan, K. Zou, S. Wu, S. Lee, Micron 36, 55 (2005)
14. F. Yakuphanoglu, S. Ilican, M. Caglar, Y. Caglar, Superlattices Microstruct. 47, 732 (2010)
15. Cullity BD: Elements of X-ray diffraction Massachusetts: Addison-Wesley; 1978,102.
16. N. Thirugnanam, H. Song, Y. Wu, Chin. J. Catal. 38, 2150 (2017)
17. N. Fifere, A. Airinei, D. Timpu, A. Rotaru, L. Sacarescu, L. Ursu, J. Alloys Compd. 757, 60 (2018)
18. L. Chanu, W. Singh, K. Singh, K. Devi, Results Phys. 12, 1230 (2019)
19. A. Al-Hajry, Ahmad Umar, Y. B. Hahn, and D. H. Kim, Superlattices Microstruct. 45, 529 (2009).
20. R. A. Nyquist and R. O. Kagel, Infrared Spectra of Inorganic Compounds, Academic Press, Inc., New York, London (1971).
21. Y. H. Ni, X. W. Wei, J. M. Hong, and Y. Ye, Mater. Sci. Eng. B 121, 42 (2005).
22. Thangavel R, Moirangthem RS, Lee WS, Chang YC, Wei PK, Kumar J. Cesium doped and undoped ZnO nanocrystalline thin films: a comparative study of structural and micro-Raman investigation of optical phonons. J Raman Spectrosc. 41(12):1594(2010)
23. Sui YR, Wu YJ, Song YP, Lv SQ, Yao B, Meng XW, Xiao L. A study on structural formation and optical properties of Zn_{1-x}Cd_xO thin films synthesized by the DC and RF reactive magnetron co-sputtering. J Alloys Compd.678:383(2016).